



Research Paper

Augmentation of heat transfer coefficient in pool boiling using compound enhancement techniques



A. Sathyabhama, Athul Dinesh*

Department of Mechanical Engineering, NITK Surathkal, Srinivasnagar 575 025, India

HIGHLIGHTS

- Compound augmentation of grooves with surface vibration was used for boiling heat transfer enhancement.
- The compound technique gave heat transfer enhancement of 78%.
- At constant amplitude, very high frequency and very low frequency did not improve the heat transfer. Effect of amplitude was significant only at low frequency.
- The bubble break-off diameter decreased by almost 36% and the bubble frequency increased by 221% in enhanced boiling.

ARTICLE INFO

Article history:

Received 7 November 2016

Revised 21 January 2017

Accepted 5 March 2017

Available online 16 March 2017

Keywords:

Enhancement

Visualization

Correlation

Grooved surface

ABSTRACT

Modern compact electronic chip design demands more efficient and innovative cooling techniques in a limited space. One such method is the immersion cooling by pool boiling heat transfer, which is a highly efficient technique when compared with conventional cooling techniques. The boiling heat transfer coefficient can be enhanced using active and passive techniques. In the present investigation grooves as passive and surface vibration as active techniques were coupled to improve the boiling heat transfer coefficient. The forced vertical vibrations were induced on the copper grooved surface with a mechanical vibrator. The frequency of vibration was varied in the range 0–100 Hz and the amplitude of vibration was varied in the range 0–2.5 mm. The compound technique gave 62% improvement in heat transfer coefficient at 300 kW/m² heat flux compared to the 29% enhancement due to grooves alone and 10% enhancement due to vibration alone. The experimental results were used to develop a modified Rohsenow correlation which predicts the experimental Nusselt number with an accuracy of ±25%. Boiling visualization was performed and the bubble parameters such as bubble departure diameter, bubble frequency and bubble growth were determined. The bubble departure diameter decreased by almost 36% and the bubble frequency increased by 221% for boiling on vibrated grooved surface.

© 2017 Elsevier Ltd. All rights reserved.

1. Introduction

The thermal management of electronic chips has become a challenge with rapidly increasing power dissipation in recent years. The passage of electric current through the electronic components makes them potential sites for excessive heating, since the current flow through a resistance is accompanied by heat generation. Continued miniaturization of electronic systems has resulted in a dramatic increase in the amount of heat generated per unit volume. The failure rate of electronic components

increases exponentially with temperature. Therefore, thermal control has become increasingly important in the design and operation of electronic equipment.

The high-power electronic components can be cooled effectively by immersing them in a dielectric liquid and taking advantage of the very high heat transfer coefficients associated with boiling. The heat transfer in immersion cooling can be further increased by the augmentation techniques namely, active techniques, passive techniques, compound techniques. Active method involves some external power input for the enhancement of heat transfer. Some examples of active methods are, surface vibration, mechanical aids, fluid vibration, electrostatic fields, injection, suction, jet impingement. Passive techniques generally use surface or geometrical modifications to the flow channel by incorporating

Abbreviations: BHTC, boiling heat transfer coefficient; CHF, critical heat flux.

* Corresponding author.

E-mail address: bhama72@gmail.com (A. Dinesh).

Nomenclature

A_f	area enhancement factor	R_{cav}	radius of the cavity mouth (m)
a	amplitude of vibration (m)	Re	Reynold's number
D	diameter of heater (m)	Re_v	vibrational Reynold's number
d	instantaneous bubble diameter (mm)	q	heat flux (kW/m^2)
d_b	bubble departure diameter (mm)	T	temperature ($^{\circ}\text{C}$)
d^*	non-dimensional bubble diameter	x	distance between thermocouples
f	frequency of vibration (Hz)		
f_b	bubble departure frequency (Hz)	<i>Greek letters</i>	
f_m	vibration frequency of the heater at which maximum heat transfer occurs	α	cavity vertex half angle
h	heat transfer coefficient ($\text{kW/m}^2\text{ }^{\circ}\text{C}$)	θ	wetting angle (radian)
K	thermal conductivity (W/m K)	θ_0	wetting angle without vibration (radian)
k	dimensionless wavenumber	τ	instantaneous growth time (ms)
Nu	Nusselt number	τ_{total}	total growth time (ms)
Pr	Prandtl number	τ^*	non-dimensional growth time
R	bubble radius (m)	ν	kinematic viscosity (m^2/s)

inserts or additional devices. They promote higher heat transfer coefficients by disturbing or altering the existing flow behaviour (except for extended surfaces) which also leads to increase in the pressure drop. In case of extended surfaces, effective heat transfer area is increased. Passive techniques hold the advantage over the active techniques as they do not require any direct input of external power. Examples of passive technique are, extended surfaces, treated surfaces, rough surfaces, displaced enhancement devices, swirl flow devices, coiled tubes, surface tension devices, additives for liquids, additives for gases. When any two or more of these techniques are employed simultaneously to obtain enhancement in heat transfer that is greater than that produced by either of them when used individually, is termed as compound enhancement. Compound techniques offer a way to further elevate heat transfer coefficients and this area of enhancement technology holds much promise for future development [1]. A variety of combinations for two or more enhancement methods or devices have been explored by some researchers. Compound technique will be effective for systems having one form of enhancement naturally. Rotating systems, which include rotor windings of large turbogenerators or electric motors, and gas-turbine blades are good examples [2]. A few different passive techniques have been applied in rotating tubes and ducts in the literature [3–9]. Many different compound schemes involving twisted-tape inserts have been considered for single-phase forced-convective and boiling applications. The heat transfer coefficients are generally enhanced to a greater extent than that with each individual technique in these cases. Some other representative examples of promising compound enhancement techniques for varied practical applications have been proposed in the literature. One example is the application of EHD fields in pool boiling of refrigerant R-134a from microfinned and treated tubes [10].

Although having been a subject of research for several decades, an expansive study on the effect of compound enhancement on boiling heat transfer is hard to find in the literature which was the incentive to pursue the current investigation. Previously many research work were carried out to study the effect of vibration/effect of surface modification alone on heat transfer, and have reported substantial enhancement in boiling heat transfer coefficient (BHTC) and critical heat flux (CHF). Works which focus on the study of compound enhancement on BHTC with induced vibration on modified surface is unavailable in the literature. So, in the present work the effect of surface vibration on boiling heat transfer over a rectangular grooved surface (GS) will be explored. Furthermore, the boiling heat transfer rate is strongly related to bubble

dynamics (i.e. bubble nucleation, growth and detachment). Several bubble parameters like bubble departure diameter, bubble departure frequency, and the growth/wait time are important in determining the nucleate boiling heat transfer coefficient. Therefore, in order to gain insight into the heat transfer mechanisms during boiling on the excited grooved surface, bubble dynamics will be discussed in this paper.

2. Experimental facility

The experimental apparatus, shown in Fig. 1 has a boiling chamber of $200 \times 200 \times 350$ mm made up of SS 316 fitted with SS 316 flanges at the top and at the bottom. The provisions for liquid charging and condenser cooling are at the top flange and for test section and drainage pipe at the bottom flange. Four circular glass windows are fitted to the side walls of boiling vessel to aid visualization. The cooling water circulates through the copper condenser coil and condenses the water vapor formed during the boiling and keeps the pressure inside the boiling chamber constant. An auxiliary heater of 500 W capacity inserted through the side wall of the boiling chamber maintains the water (the working fluid used in the current study) at constant saturation temperature during the experimentation. Another electrical heating element of 500 W capacity is inserted in a cylindrical copper rod of 15 mm diameter to give heat input to the test surfaces as shown in Fig. 2. The rod heater is mounted vertically from the bottom of the boiling vessel. High temperature nylon insulators are wrapped around the copper heater to reduce the unwanted heat losses. On the top of the heater rod the replaceable circular test piece of 19 mm diameter and 7 mm thickness is placed (Fig. 2). The replaceable test piece has a groove of 15.7 mm diameter and 3 mm depth which exactly fits on the 15 mm diameter heater rod. Thermal grease is used in between the test surface and the heater rod to reduce the contact resistance. The boiling takes place on top of the test surface when the experiment is done. Details of grooved test surface are given in Fig. 3. Grooves of 3 mm depth, 2 mm width with fin thickness of 1 mm were cut on the test surface.

A wattmeter connected to the heating element measures the power supplied to it. Three thermocouples are placed inside the boiling vessel, out of which two are in the liquid pool to measure the saturation temperature of the liquid and one is in the vapor region for the vapor temperature measurement. The liquid and vapor temperatures recorded by these thermocouples confirm that the system is being maintained at the saturation state during the

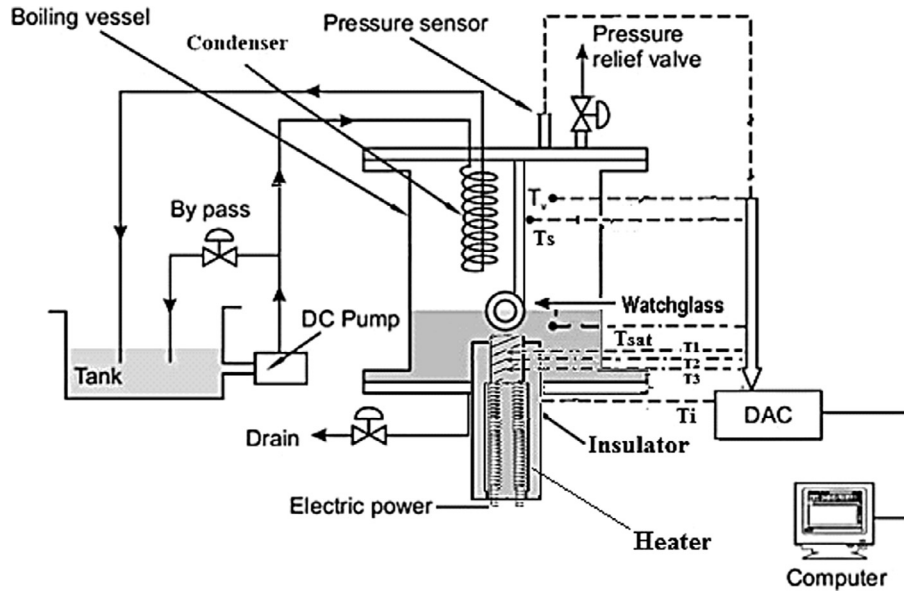


Fig. 1. Schematic of experimental facility.

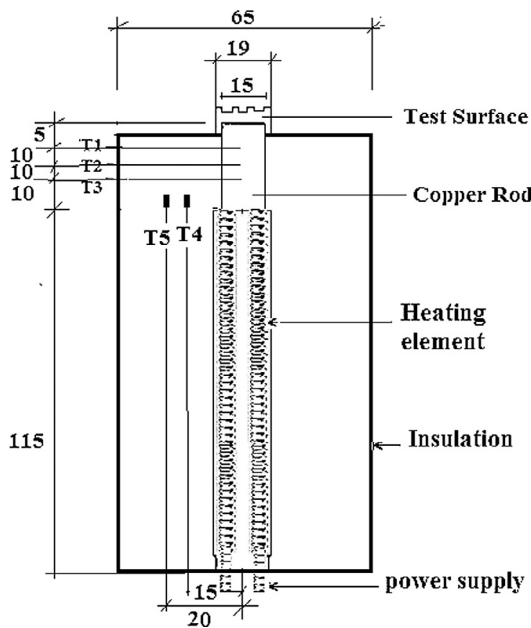
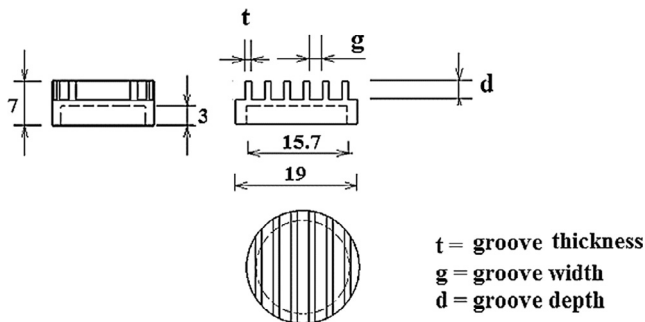


Fig. 2. Details of heater assembly.



Note: All dimensions are in mm

Fig. 3. Details of grooved surface (GS).

experiment. Another three thermocouples are provided along the length of the heater rod at a distance of 10 mm each. These thermocouple readings are used to calculate the temperature gradient and the heat flux. The test piece surface temperature is calculated by extrapolation. Two thermocouples present on the insulation at a radial distance of 15 mm and 20 mm give readings which are used to calculate the radial heat loss. A mechanical vibrator excites the heater rod and the vibration of this exciter is controlled using a power oscillator. The exact values of vibration parameters like frequency and amplitude is measured using an accelerometer.

2.1. Experimental procedure

Initially the boiling vessel was evacuated using a vacuum pump. Then the boiling vessel was filled with distilled water. The pressure of the boiling vessel was then noted from the display unit. The amount of water used in all the experiments was the same. Auxiliary heater was switched on to bring the water to saturation state. When the water reached saturation state, the tests were started by giving heat input to the test surface. The magnitude of this heat input was known from the wattmeter. After steady state was reached, the saturation temperature and the test surface temperature were noted down and the procedure was repeated for different heat flux values. The set pressure was maintained constant throughout an experiment by the combination of the cooling water pump, pressure transducer and a proportional integral derivative (PID) pressure controller. The PID senses the pressure level in the boiling chamber through pressure transducer and compares it with the set value fed to it by the researcher. To go from a higher pressure level to a lower pressure level, the PID sends a signal to cooling water pump to open the suction line and pump water through the condenser coils. To obtain data on vibration effects, the same procedure was repeated but with the vibration exciter switched on. Experiments were conducted by varying the frequency and amplitude of vibration.

All the data were collected and systematically fed into a spreadsheet document. Mathematical relations were used to obtain required results. These variables were graphically plotted and were used for comparison and analysis. Local heat transfer coefficient between the surface and the water was calculated by using the Eq. (1).

$$h = \frac{q}{T_w - T_s} \quad q = -K \frac{dT}{dx} \quad (1)$$

Here, T_s is the saturation temperature of the water at the corresponding pressure, and T_w is the test surface temperature.

2.2. Visualization of the boiling process

Fig. 4 shows the photographic view of pool boiling visualization facility. High speed camera (AOS Promon 501) was used for visualization of pool boiling process. The camera was positioned in front of the sight glass. A concentrated light source was placed in front of another sight glass opposite to the camera to give uniform illumination to the test surface. A gigabyte Ethernet cable which acts as data logger connects the camera with PC for data transfer. Nikon lens 50 mm FL, f1.4D was used. Promon studio viewer software interfaces camera with PC. This user interface software was used to control triggering and recording the videos and it was also used to set the shutter speed, pixel size, and frame rate of the videos to be captured. The camera can record live scenes of boiling phenomenon on the test surface at a frame rate of 1000 frames per second (fps) with resolution of 320×240 pixels. These recorded videos were played back and as per the requirement, the scene length was marked frame by frame and were converted into sequence of images which were processed in Matlab image processing tool to determine bubble diameter in pixel as a function of time. A reference object of known size was placed inside the boiling chamber. A snapshot was taken from the same focal distance and the pixel size was measured. This was used to find out the conversion factor. Thus linear size of bubble is calculated by using the above said conversion factor.

2.3. Experimental uncertainty

The uncertainty in temperature measurement is ± 0.1 °C. Uncertainty in distance measurement is ± 0.1 mm. Kline and McClintock [11] method was used to estimate the uncertainty for the derived quantities. The resulting maximum uncertainty in the heat flux was 1.55%. The maximum uncertainty in the wall superheat values was 0.44%. The maximum uncertainty in the BHTC was 2.57%. The maximum uncertainty in bubble frequency was 2.78% and uncertainty in bubble diameter measurement was 0.05 mm.

3. Results and discussion

The aim of the present study is to determine the influence of compound enhancement on BHTC of water at atmospheric pressure. The results obtained were plotted as boiling curves (heat flux versus wall superheat) and BHTC versus heat flux graphs. The geometrical details of the test surfaces used is listed in Table 1. The experiments were done in a particular order to observe the influence of addition of each type of enhancement technique on the BHTC. Initially the experiment was conducted with plane surface (PS). Next, the PS was excited with 2 Hz frequency and 1 mm amplitude. This experiment gave the results which demonstrated the effect of active enhancement technique alone. The next experiment was done with GS (surface modification), which showed the influence of passive enhancement technique alone. Finally, GS was made to vibrate at 2 Hz frequency and 1 mm amplitude. The results displayed the effect of compound enhancement on the BHTC. The results of all the above said experiments are shown in Figs. 5a and 5b. It can be observed that the test surface shows best heat dissipation when compound enhancement technique is used. The compound technique gave 62% improvement in heat transfer coefficient at 300 kW/m^2 heat flux compared to the 29% enhancement due to grooves alone and 10% enhancement due to vibration alone. Increase in bubble emission due to increased active nucleation sites because of grooves and early removal of bubbles due to induced vibration are the reasons for this enhancement. Any effort to remove the bubbles when they are smaller in size would enhance the heat transfer since the heat transfer coefficient for a bubble decreases as it grows.

3.1. Effect of frequency of vibration

The experiments were later carried out with only GS to study the effect of frequency and amplitude of vibration. Figs. 6a–6d depict the results of experiments done at a constant amplitude of 1 mm with varying frequency. It can be perceived from these figures that heat transfer deteriorates with increase in frequency up to 10 Hz. With further increase in frequency heat transfer coefficient intensifies significantly. It is noteworthy that as the frequency was increased above 25 Hz, the heat transfer from GS deteriorated but was always better than the stationary condition of GS. Further experiments with frequencies above 100 Hz were

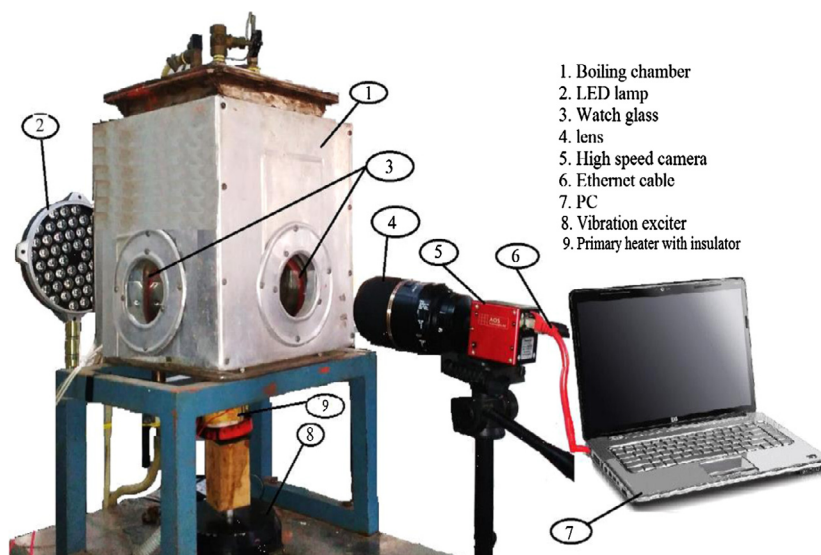




Fig. 4. Visualization facility.

Table 1
Geometrical details of test surfaces.

Surface type	Photo	Groove depth (mm)	Fin thickness (mm)	Groove width (mm)	Area enhancement factor	Total thickness (mm)	Diameter (mm)
Plain surface (PS)		-	-	-	1.0	7	19
Grooved surface (GS)		3	1	2	1.55	7	19

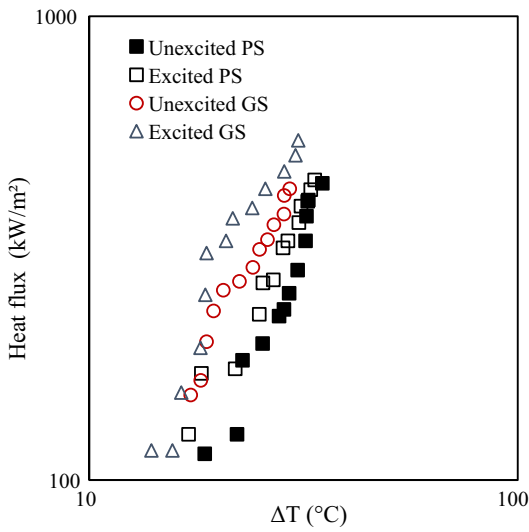


Fig. 5a. Effect of enhancement technique on boiling curve.

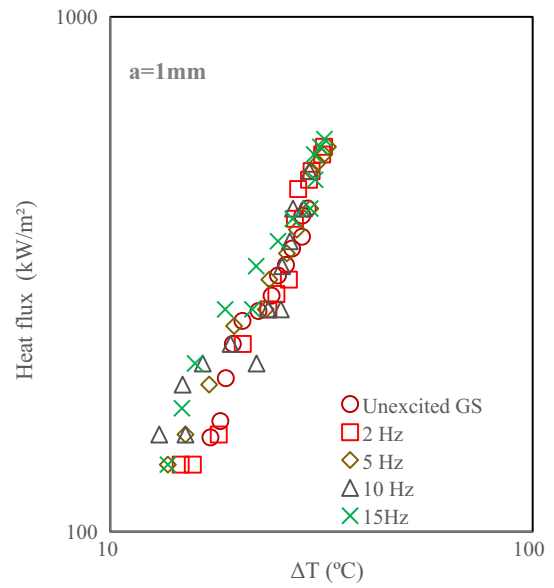


Fig. 6a. Effect of excitation frequency (<20 Hz) at 1 mm amplitude on the boiling curve.

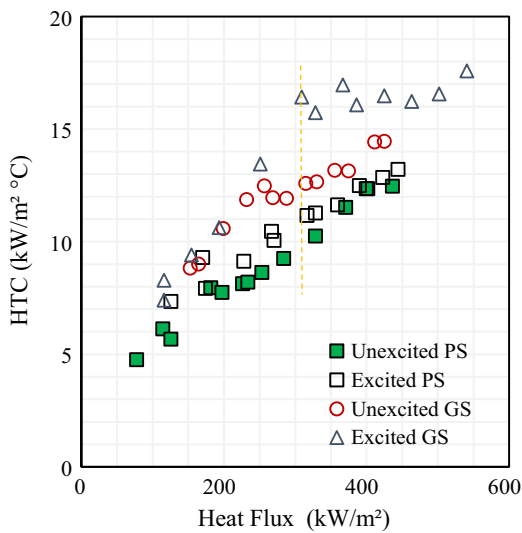


Fig. 5b. Effect of enhancement technique on BHTC.

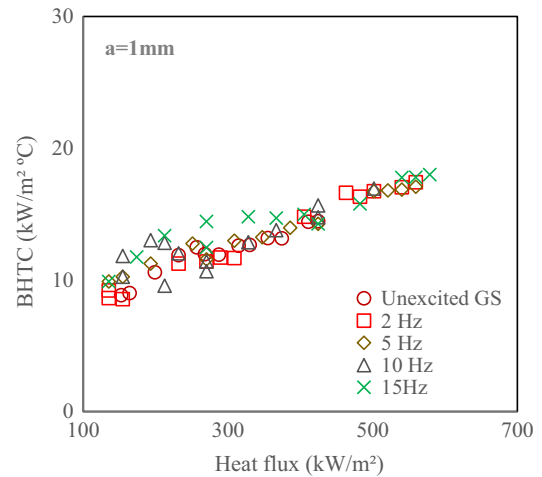


Fig. 6b. Effect of excitation frequency (<20 Hz) at 1 mm amplitude on the BHTC.

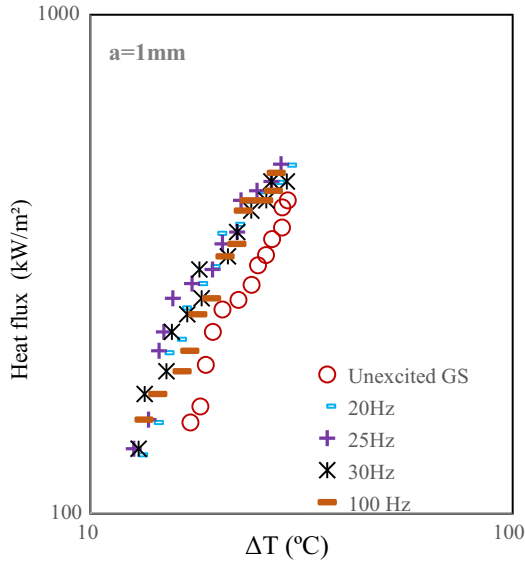


Fig. 6c. Effect of excitation frequency (>20 Hz) at 1 mm amplitude on the boiling curve.

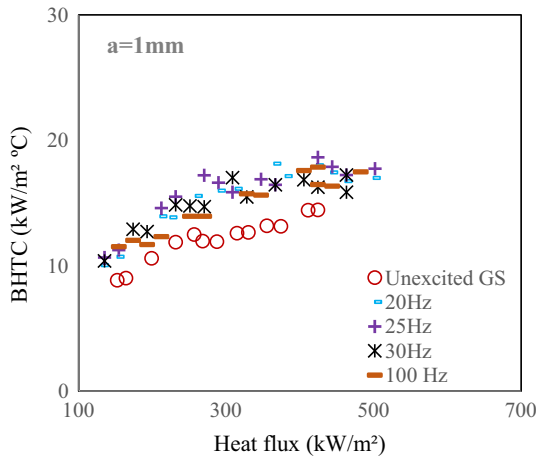


Fig. 6d. Effect of excitation frequency (>20 Hz) at 1 mm amplitude on the BHTC.

discontinued since there was no notable improvement in the heat dissipation from the GS. The possible reason can be that, as the frequency increase to a much higher value, the fluid above the test surface does not get enough time to get heated up. The fluid chunks are driven away by the fast moving GS which negatively affects the heat flow to the fluid as suggested by Navruzov and Prisyakov [12]. At very low frequencies, the increased bubble rate due to grooves damp the vibration. It may also be observed that at higher heat flux values, all the curves tend to merge indicating that the effect of vibration is prominent in the lower range of nucleate boiling. This is because, in lower heat flux boiling regions, the transfer of heat takes place primarily through boundary layer and the external agitation caused by the vibration disturbs the thermal boundary layer enhancing the BHTC. At higher heat flux boiling regions, the heat transfer by latent heat transport is dominant and vibration has no effect on augmentation of BHTC.

3.2. Effect of amplitude of vibration

Experiments were conducted by exciting GS at different amplitudes at constant frequencies 2 Hz, 5 Hz and 10 Hz. The amplitudes

chosen were 1 mm, 2 mm and 2.5 mm owing to the limitation of the mechanical vibrator. Figs. 7–9 show the results obtained from these nine sets of experiments. At 2 Hz and 5 Hz vibrational frequency, the escalation of heat transfer with the increase in amplitude was the most significant. The overall increase in the heat transfer was around 75% and the increase in BHTC values was about 40%. On the contrary, the hike in the heat dissipation from GS at 10 Hz frequency and different amplitudes was miniscule. Chekanov and Kul'gina [13] also observed that the effect of amplitude was significant at low frequencies of vibration. It means that the heat transfer intensification obtained by inducing higher frequencies of vibration can also be achieved at lower frequencies, but by increasing the amplitude of vibration.

4. Boiling visualization

The boiling heat transfer is intimately linked to bubble dynamics. Bubble nucleation, growth, frequency and detachment are the governing factors which affect the boiling heat transfer. Therefore, in order to gain an insight into the heat transfer mechanisms during boiling an understanding of the bubble dynamics is required. In the current study, the effect of compound enhancement of boiling on various bubble parameters were studied by boiling visualization using a high speed camera. These results are discussed in the following sections.

4.1. Effect of compound enhancement on bubble life cycle

Bubble life cycle is the periodic succession of events from nucleation of a bubble at its nucleation site, growth of this bubble until its departure, and rise of the bubble until it reaches the free surface of water. Figs. 10–12 show the bubble nucleation, growth and departure pattern under different test conditions. Frames were captured at an interval of 1 ms (ms) using high speed camera. It can be observed that the bubble growth over stationary PS has the longest duration of 12 ms. After the bubble reached its departure diameter it stayed on the test surface for almost 1 ms. The

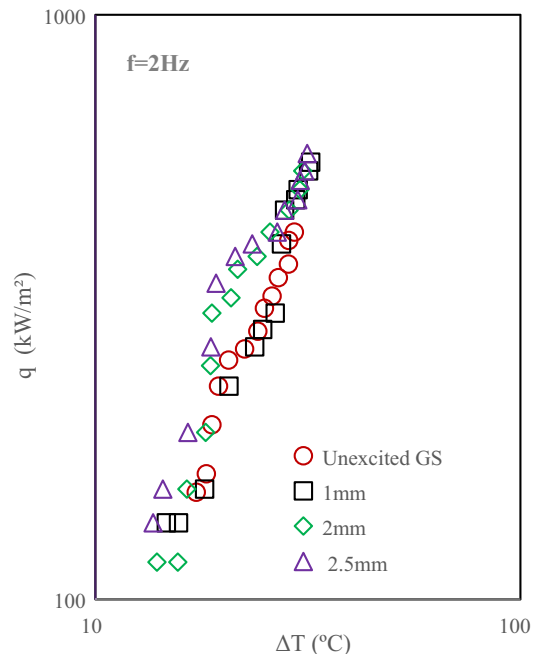


Fig. 7a. Effect of excitation amplitude at 2 Hz frequency on the boiling curve.

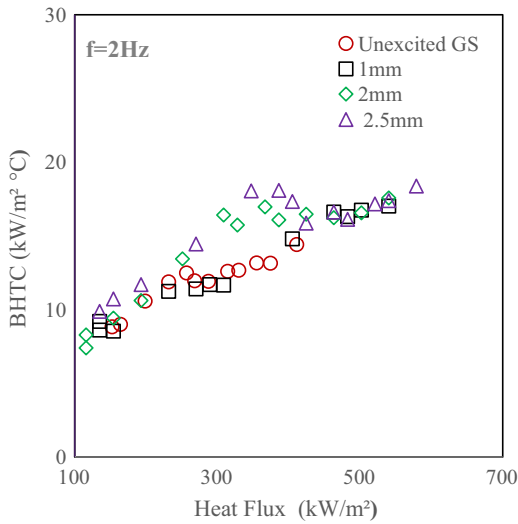


Fig. 7b. Effect of excitation amplitude at 2 Hz frequency on the BHTC.

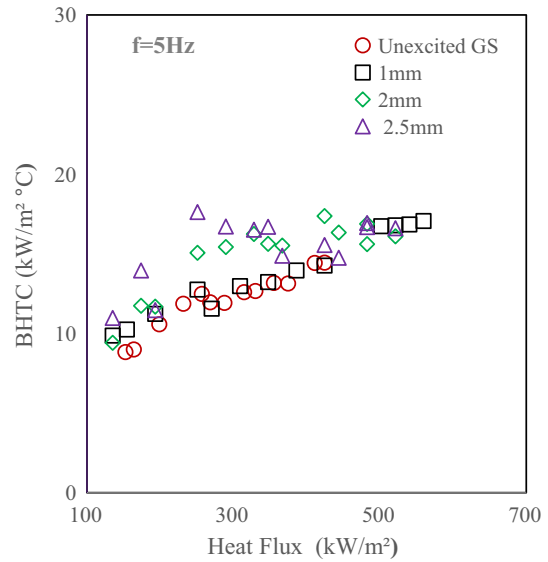


Fig. 8b. Effect of excitation amplitude at 5 Hz frequency on the BHTC.

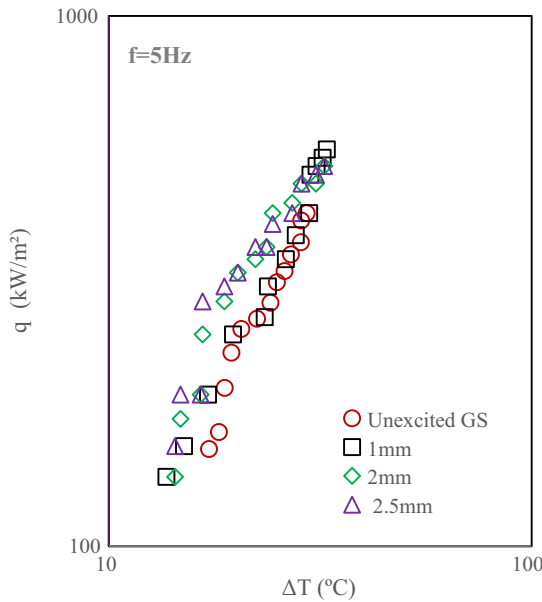


Fig. 8a. Effect of excitation amplitude at 5 Hz frequency on the boiling curve.

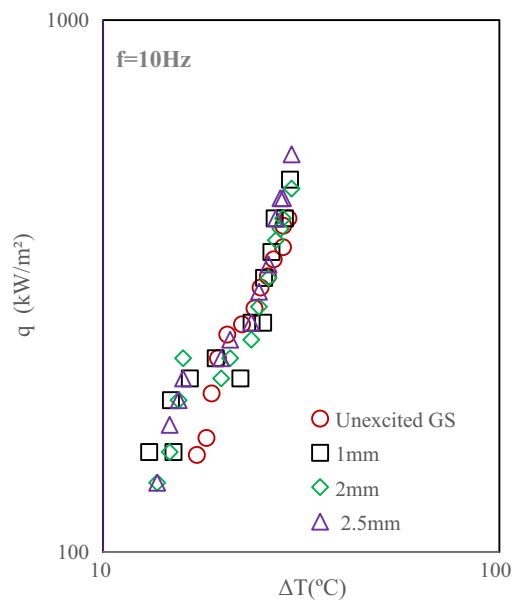


Fig. 9a. Effect of excitation amplitude at 10 Hz frequency on the boiling curve.

bubble departed from excited PS in 8 ms, which was quicker compared to the bubble growth over stationary PS. This can be attributed to the disturbance caused by the vibration to the bubble growth which causes the bubble to depart faster.

Most of the bubbles had nucleated from the groove edge over the GS. They slide along the groove and quickly depart after 6 ms. Excitation of GS reduced the bubble growth time further down to 5 ms. The interfering action of growing bubbles due to increase in the number of potential nucleation sites and faster removal of bubble from the test surface due to vibration are the reasons for reduction in bubble growth time.

4.2. Bubble growth

The main possible consequence on the bubble growth of the compound enhancement technique is the alteration of the vapor

production rate, causing a modification of the bubble growth rate and possibly of the bubble departure diameter. The vapor production rate is strongly related to the temperature gradient in the fluid surrounding the bubble, and thus to the heat flux and wall super heat [14]. Hence, in the current study the wall superheat and heat flux were chosen as the reference parameters. The growth curves shown in Fig. 13 for the unexcited PS have been normalized by dividing the time by the total growth time ($\tau^* = \tau/\tau_{total}$), and bubble diameter by bubble departure diameter ($d^* = d/d_b$). It can be observed that the pattern of the bubble growth is almost similar at all heat fluxes. Fig. 14 depicts the growth curves for different test cases at constant heat flux of 150 kW/m². The instantaneous bubble diameters are plotted as a function of square root of time. The entire growth period is heat transfer controlled for all the cases, since the instantaneous bubble diameter is proportional to square root of time. Growth rate is greatest and fastest for the unexcited

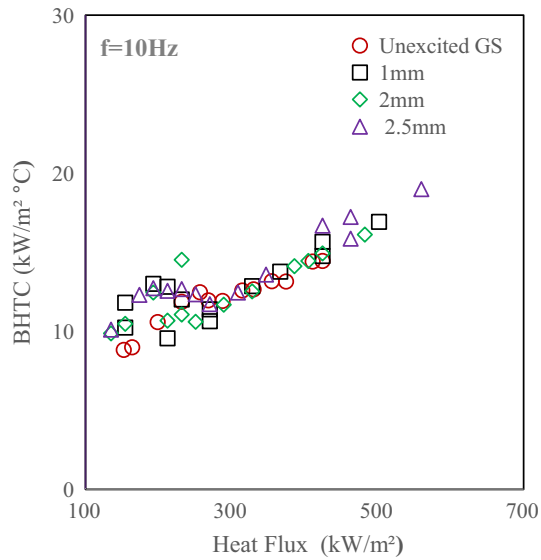


Fig. 9b. Effect of excitation amplitude at 10 Hz frequency on the BHTC.

PS. Quicker growth rate and smaller diameter can be observed for all other case as expected.

4.3. Waiting time

The maximum waiting time of bubbles was 3 ms over the unexcited PS and 2 ms over the excited PS as seen in Fig. 15(a) and (b) respectively. Moreover, the waiting period of bubbles was diminutive at high heat fluxes as bubble growth initiated faster on the potential active nucleation site which was also observed by Nangia and Chon [15]. Waiting period of bubbles generated from GS could not be measured owing to limitations of camera specification.

4.4. Bubble departure diameter

Bubble departure diameter or bubble break-off diameter is the diameter when the bubble detach from the heating surface. The variation in bubble departure diameter is shown in Fig. 16 and percentage of variation in Table 2. In GS the heat transfer to the surrounding fluid is more due to the increased wetted area, which makes the liquid less dense near the bubble nucleation sites. This

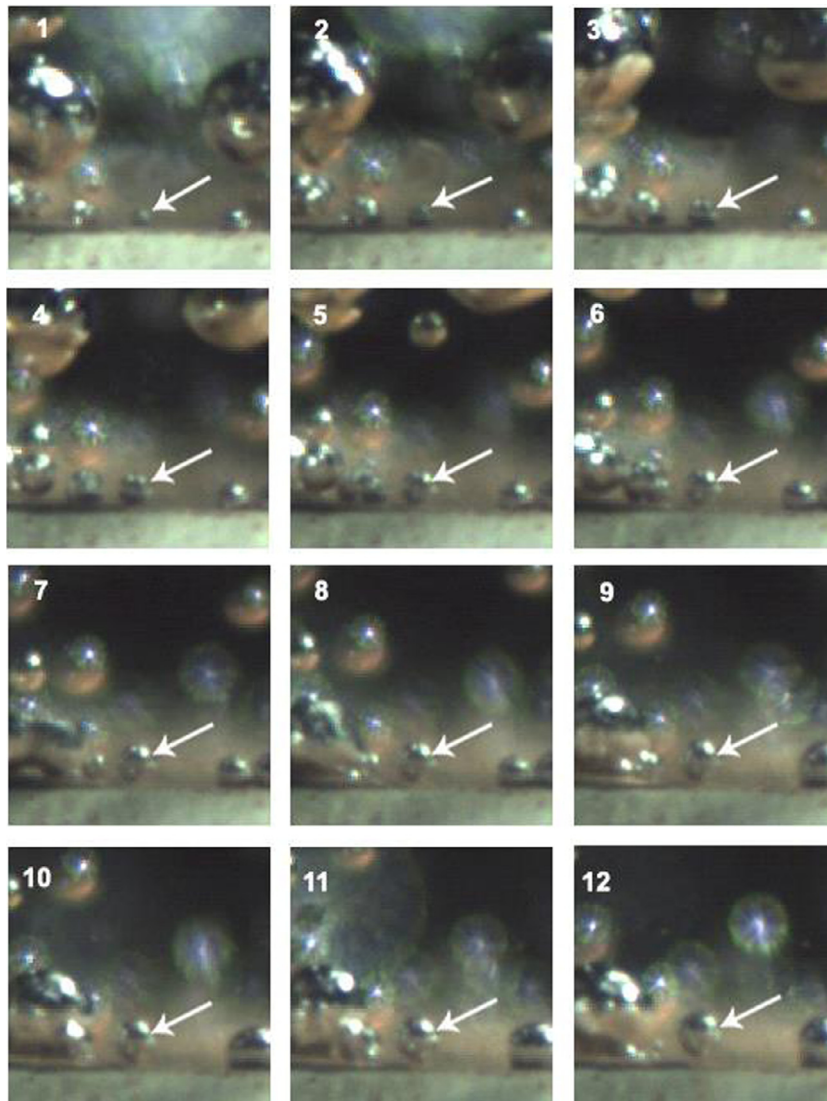


Fig. 10. Bubble growth over stationary PS at 200 kW/m² heat flux.

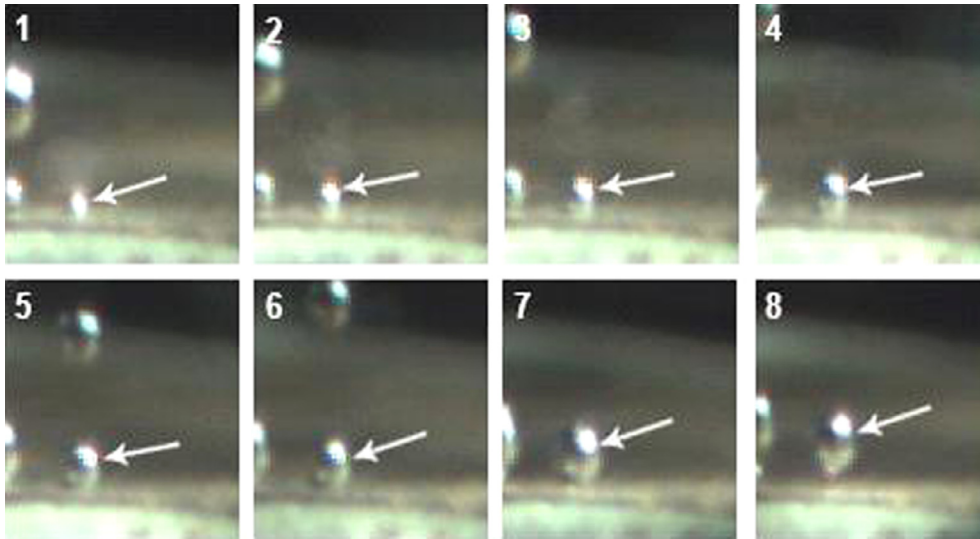


Fig. 11. Bubble growth over excited PS at 200 kW/m² heat flux.

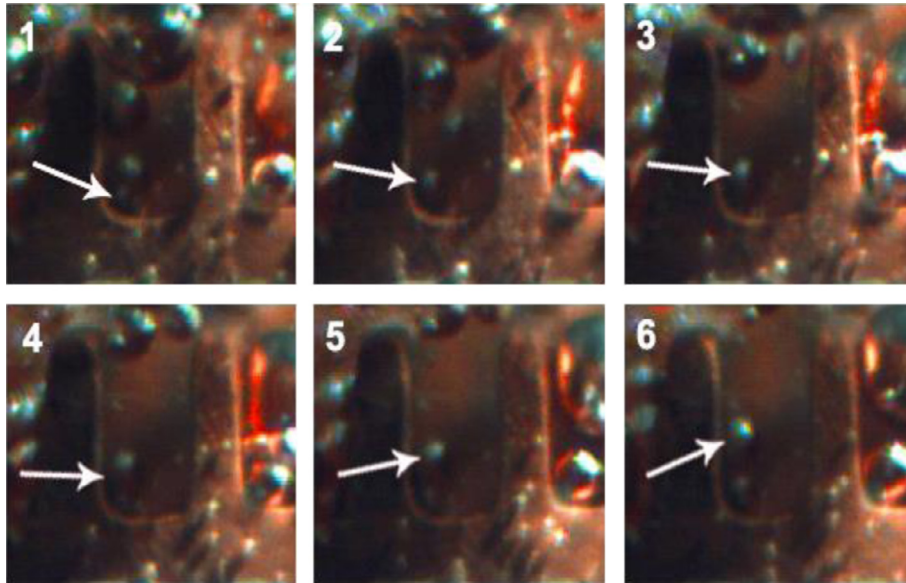


Fig. 12a. Bubble growth over stationary GS at 200 kW/m² heat flux.

causes the nucleating bubble to depart at a smaller bubble departure diameter. When vibration is induced to the test surface, bubbles are forcefully shaken off from the test surface before it reaches its typical departure diameter. This increases bubble generation, because a potential bubble nucleation site becomes open as bubbles break off faster. Moreover, greater bubble production improves the heat dissipation to the surrounding water. At very low wall superheats the bubble departure diameter is a function of the buoyancy and surface tension forces only, with an increase in the wall temperature, the surface tension reduces (for most fluids) which results in a decrease in the departure diameter.

Since the bubble behaviour is highly random in nature, statistical analysis is done. Figs. 17–20 display the statistical analysis of bubble break-off diameter and it can be observed that the diameters at break-off follow normal patterns of distribution as

witnessed by Nangia and Chon [15]. It can be also perceived that this pattern of distribution is similar for all the experimental conditions i.e. with and without the enhancement of the test surface.

4.5. Bubble frequency

It defines the total time elapsed for one bubble cycle commencing from its nucleation to departure. The bubble frequency of 30 bubbles generated from the same nucleation site is used to calculate the mean bubble frequency over a particular test surface. As expected, the bubble frequency over the test surface was maximum when the compound enhancement technique was used (Fig. 21). The increased wetting area of test surface and induced vibration are the reason for this rise of bubble frequency from typical boiling over the plain surface (Table 3).

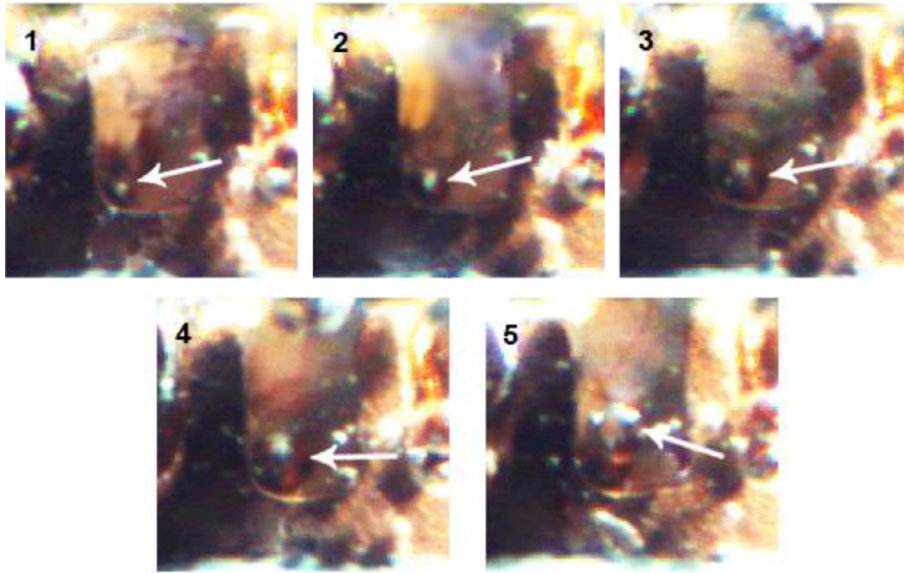


Fig. 12b. Bubble growth over excited GS at 200 kW/m² heat flux.

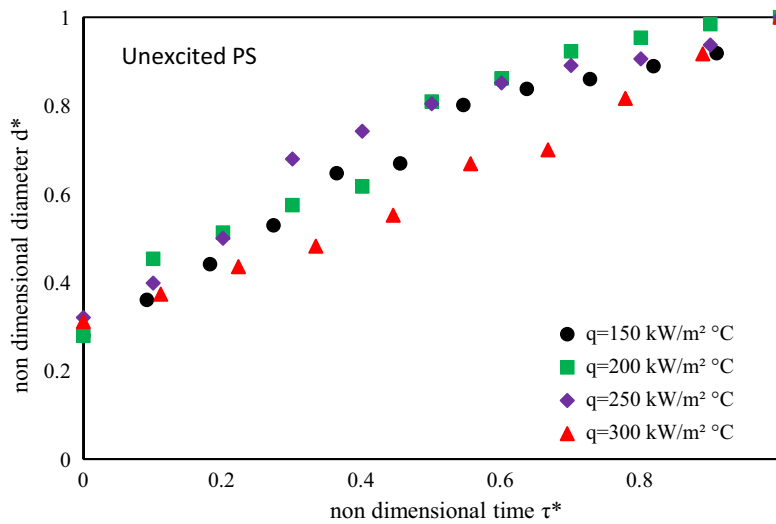


Fig. 13. Bubble growth curves for different heat fluxes of unexcited PS.

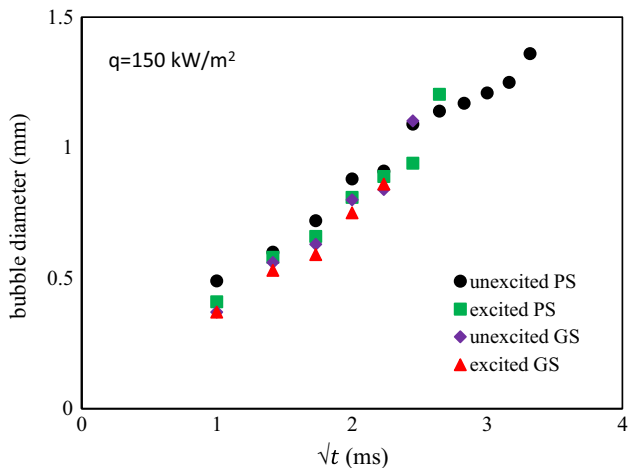


Fig. 14. Bubble growth curves for different test surfaces at 150 kW/m² heat flux.

5. Extremum frequency

Extremum frequency is the frequency of vibration of the test surface at which the maximum heat transfer occurs. Eq. (2) is used for finding the extremum frequency

$$f_m = f_b \left[k\pi - \arcsin \left(\frac{\theta_0 R_{cav} \sin(\alpha - \theta_0)}{f_b \cos^2(\alpha - \theta_0)} \right) \right] \quad (2)$$

where R_{cav} is the radius of the cavity mouth $R_{cav} = R \cos(\alpha - \theta)$.

This equation was developed by Prisnyakov and Prisnyakov [16] who evaluated the influence of vibration on the internal characteristics of boiling. The main idea of the hypothesis was that the vibrations exert an influence through the wetting angle, which changes as the bubble moves with displacement of the heating surface. In the present investigation this formula was used to check whether the experimental data matched with the theoretical data. The wetting angles were obtained from the images processed from

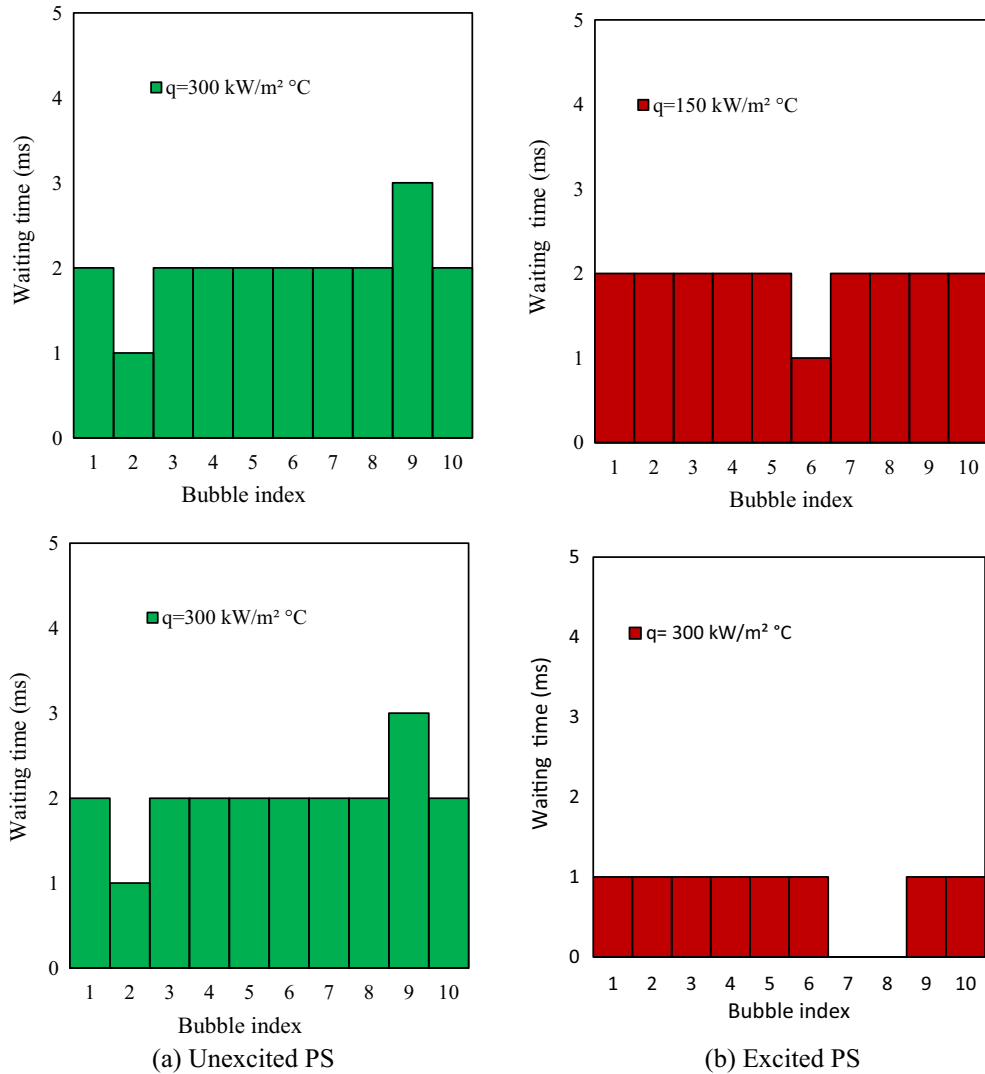


Fig. 15. Fluctuations in waiting period of bubbles.

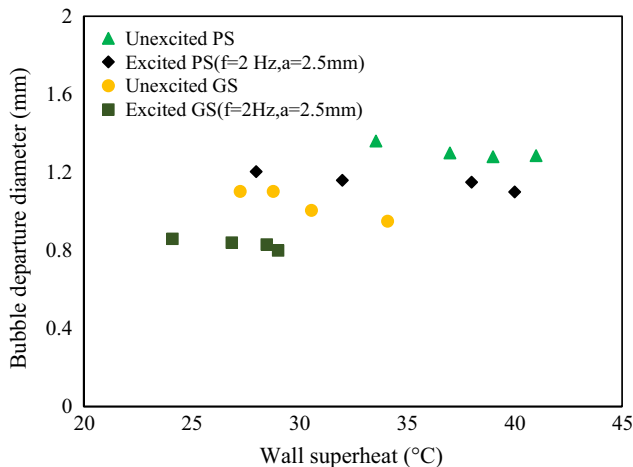


Fig. 16. Variation of bubble departure diameters.

6. Development of correlation from the experimental data

A correlation for Nusselt number was developed (Eq. (2)), based on nucleate pool boiling correlation by Rohsenow [17], using the power law regression method on the experimental data. The modified correlation has two new non dimensional variables, vibrational Reynolds number (Re_v) and area enhancement factor (A_f) to include the effect of vibration and surface modification. Properties of water were taken at saturation temperature. The modified Rohsenow correlation is:

$$Nu = 0.18783 (Re)^{0.3687} (Pr)^{1.929} (Re_v)^{0.033} (A_f)^{9.5489} \tag{3}$$

where $Re_v = \frac{2\pi f D a}{\nu}$.

The developed correlation predicted the Nusselt number with an accuracy of $\pm 25\%$ in the investigated range of heat flux, amplitude and frequency of vibration in the present experimental work as shown in Fig. 22.

7. Conclusions

In the present investigation both active and passive technique were coupled to improve the heat transfer coefficient. The grooves on the copper boiling surface was the passive enhancement technique and boiling surface vibration was the active enhance-

boiling visualization. Calculations from this formula gave results close to experimental ones, i.e. the frequency at which the maximum heat transfer occurs is 25 Hz.

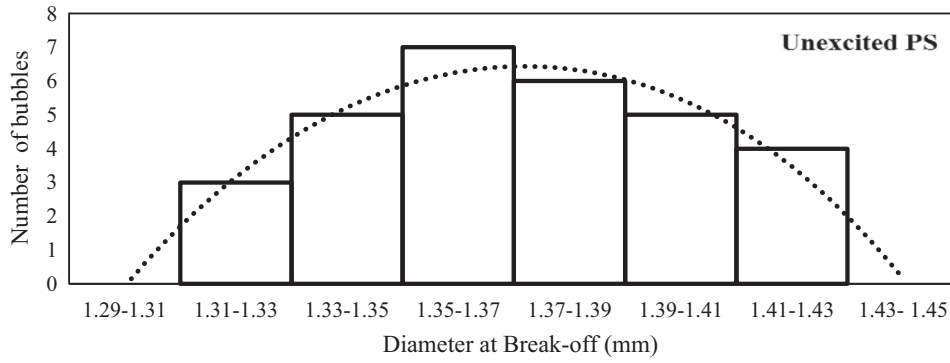


Fig. 17. Variations in diameter at break – off over unexcited PS.

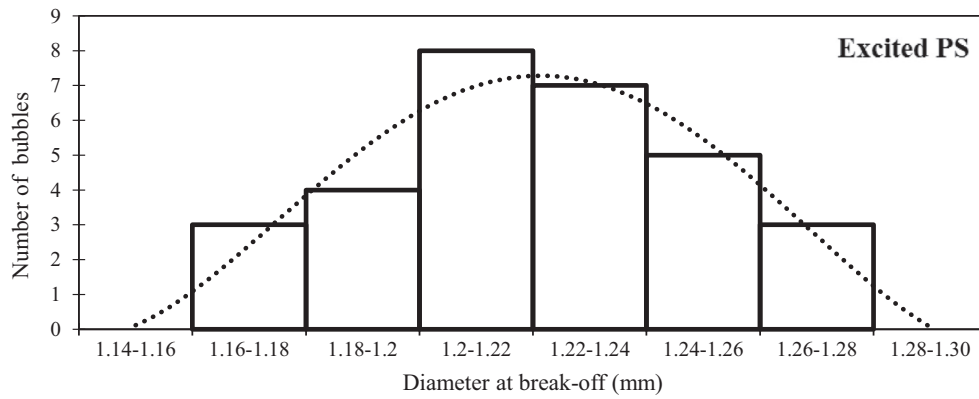


Fig. 18. Variations in diameter at break – off over excited PS.

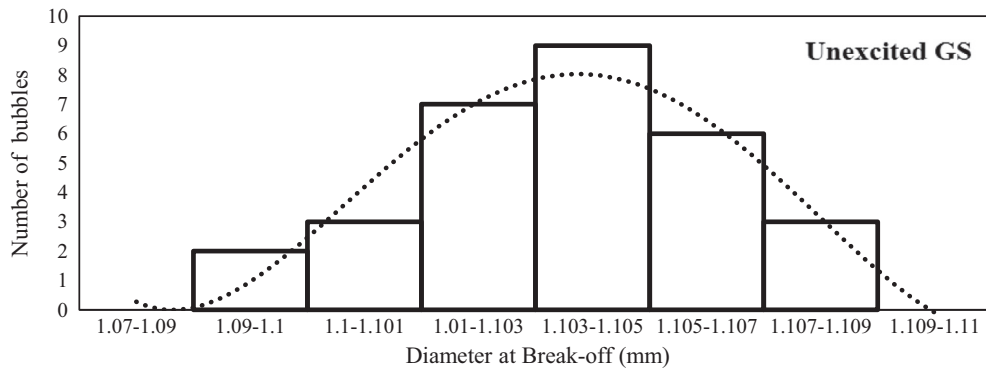


Fig. 19. Variations in diameter at break – off over unexcited GS.

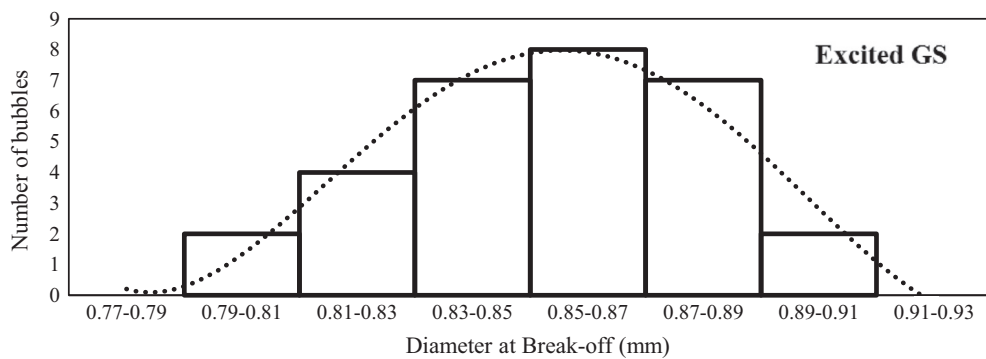


Fig. 20. Variations in diameter at break – off over excited GS.

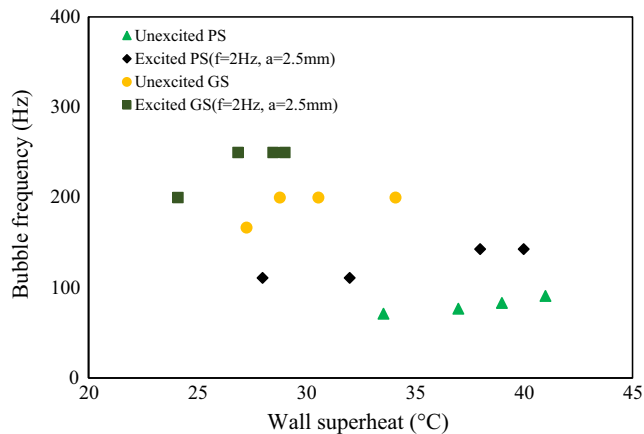


Fig. 21. Variation of bubble frequency.

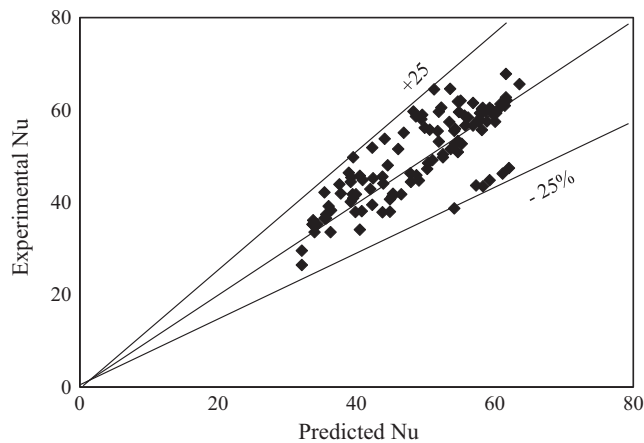


Fig. 22. Comparison between experimental and predicted Nusselt number.

Table 2
Percentage of decrease in bubble departure diameter.

Type of enhancement used	Average values of percentage of decrease in Bubble departure diameter
Excited PS at 2 Hz frequency and 2.5 mm amplitude	12%
Unexcited GS	20%
Excited GS 2 Hz frequency and 2.5 mm amplitude	6%

Table 3
Percentage of increase in bubble frequency.

Type of enhancement used	Average values of percentage of increase in bubble frequency
Excited PS at 2 Hz frequency and 2.5 mm amplitude	42%
Unexcited GS	214%
Excited GS 2 Hz frequency and 2.5 mm amplitude	221%

ment technique used. The frequency was varied in the range 0–100 Hz and the amplitude of vibration was varied in the range 0–2.5 mm for lower frequencies, 2 Hz, 5 Hz and 10 Hz. The following conclusions were drawn from the present study:

- The compound technique gave heat transfer enhancement of 62%. This can be attributed to enhanced bubble nucleation from the grooved surface and quick bubble departure from the test surface due to induced vibration.
- At constant amplitude, very high frequency and very low frequency did not improve the heat transfer. Effect of amplitude was significant only at low frequency.
- The bubble break-off diameter decreased by almost 36% and the bubble frequency increased by 221% in enhanced boiling. Bubble diameter at each stages of bubble growth decreased in enhanced boiling when compared to typical boiling.
- The extremum frequency of test surface excitation at which the maximum heat transfer occurs was found to be approximately 25 Hz, both experimentally and theoretically.
- The modified correlation predicted the Nusselt number with an accuracy of $\pm 25\%$.

Funding

This work was funded by the Department of Science and Technology, India (SR/S3/MERC-0009/2010).

References

- [1] A.E. Bergles, Enhancement of pool boiling, *Int. J. Refrig.* 20 (8) (1997) 545–551.
- [2] R.M. Manglik, Heat transfer enhancement, in: A. Bejan, A. Kraus (Eds.), *Heat Transfer Handbook*, John Wiley & Son, Hoboken, New Jersey, 2003, pp. 1029–1130.
- [3] M. Muralidhar Rao, V.M.K. Sastri, Experimental investigation of fluid flow and heat transfer in a rotating tube with twisted-tape inserts, *Heat Transfer Eng.* 16 (2) (1995) 19–28.
- [4] G.J. Hwang, S.C. Tzeng, C.P. Mao, C.Y. Soong, Heat Transfer in a radially rotating four-pass serpentine channel with staggered half-V rib turbulators, *J. Heat Transfer* 123 (1) (2001) 39–50.
- [5] H. Iacovides, D.C. Jackson, G. Kelemenis, B.E. Launder, Y.M. Yuan, Flow and heat transfer in a rotating U-bend with 45° ribs, *Int. J. Heat Fluid Flow* 22 (3) (2001) 308–314.
- [6] Y.L. Lin, T.I.P. Shih, M.A. Stephens, M.K. Chyu, A numerical study of flow and heat transfer in a smooth and ribbed U-duct with and without rotation, *J. Heat Transfer* 123 (2) (2001) 219–232.
- [7] A. Murata, S. Mochizuki, Large eddy simulation of heat transfer in an orthogonally rotating square duct with angled rib turbulators, *J. Heat Transfer* 123 (5) (2001) 858–867.
- [8] S. Acharya, R.G. Hibbs, Y. Chen, D.E. Nikitopoulos, Mass/heat transfer in a ribbed passage with cylindrical vortex generators: the effect of generator-rib spacing, *J. Heat Transfer* 122 (4) (2000) 641–652.
- [9] V. Eliades, E.D. Nikitopoulos, S. Acharya, Mass-transfer distribution in rotating, two-pass, ribbed channels with vortex generators, *J. Thermophys. Heat Transfer* 15 (3) (2001) 266–274.
- [10] J. Darabi, M.M. Ohadi, S.V. Dessiatoun, Compound augmentation of pool boiling on three selected commercial tubes, *J. Enhanced Heat Transfer* 7 (5) (2000) 347–360.
- [11] S.J. Kline, F.A. McClintock, Describing uncertainties in single-sample experiments, *Am. Soc. Mech. Eng.* 75 (1953) 3–8.
- [12] Yu. V. Navruzov, V.F. Prisyakov, Heat-transfer processes in single and two phase systems under vibration actions. Dep. at VINITI. (1987), 1867–V87.
- [13] V.V. Chekanov, L.M. Kul'gina, Effect of heater vibration on the boiling process, *Inzh.-Fiz. Zh.* 30 (1) (1976) 44–48.
- [14] S. Siedel, *Bubble Dynamics and Boiling Heat Transfer: A Study in the Presence and in the Presence of Electric Fields* PhD thesis, Institute of applied Sciences, Lyon, 2011.
- [15] K.K. Nangia, W.Y. Chon, Some observations on the effect of interfacial vibration on saturated boiling heat transfer, *AIChE J.* 13 (5) (1967) 872–876.
- [16] V.F. Prisyakov, K.V. Prisyakov, Action of vibrations on heat and mass transfer in boiling, *J. Eng. Phys. Thermo Phys.* 74 (4) (2001) 1015–1023.
- [17] W.M. Rohsenow, *A Method of Correlating Heat Transfer Data for Surface Boiling of Liquids*, Cambridge Mass MIT Division of Industrial Cooperation, 1951.